Powder Metallurgy and Metal Ceramics, Vol. 47, Nos. 1-2, 2008

COHESIVE ENERGY, PROPERTIES, AND FORMATION ENERGY OF TRANSITION METAL ALLOYS

M. A. Turchanin and P. G. Agraval

UDC 544.142.5:536.653:546.302

The cohesive energy of transition metals and its contributions related to the s- and d-electrons are calculated. The correlation of interatomic bonding strength, molar volume, and compressibility of transition metals with cohesion energy and corresponding contributions to it is shown. It is demonstrated that the s-electrons play an important part in the cohesion of transition metals. The main contributions to the formation energy of disordered alloys of copper with transition metals are calculated using the tight-binding approach. The results obtained are in qualitative agreement with experimental data on the thermodynamic properties of Cu–3d-metal systems.

Keywords: *cohesive energy, tight-binding approach, transition metals, copper-based alloys, formation enthalpy of alloy.*

In condensed state, atoms are held together by cohesive forces, which are the total forces exerted by an atom on its nearest neighbors. In most cases, it is very difficult to measure these forces because ultimate strength and elastic limit depend on the imperfection of samples in mechanical tests. Therefore, various physical properties associated with the cohesive forces and characterizing, in a way, the strength of interatomic bonds in a crystal are used as measures of these forces among atoms in a crystal lattice. These characteristics include various thermodynamic, elastic, and thermal constants of which the most important are sublimation heat, atomization energy, melting point, elastic modulus, Debye characteristic temperature, and thermal expansion coefficients [1].

Since elucidating the physical and chemical nature of interatomic interaction and cohesive forces in transition metals and their alloys is of great importance for developing the theory of condensed phases and modern physical metallurgy, it appears expedient to try to asses their cohesive energy within the available chemical binding models.

COHESIVE ENERGY AND PROPERTIES OF TRANSITION METALS

It was shown in [2–4] that the cohesive energy of transition metals is high due to the band energy of *d*-electrons and that the change of the energy along transition series may be associated with increased filling of the *d*-band. According to [2, 4, 5], the tight-binding model uses simple summation of one-electron cohesive energies to calculate the cohesive energy of a transition metal due to overlapping of *d*-electrons:

$$E_d = \int_{B_d}^{E_f} (E_d - E) n_d(E) dE \,, \tag{1}$$

where E_d is the cohesive energy due to *d*-electrons; E_f is the Fermi energy reckoned from the conduction-band bottom; E_d is the energy of the atomic *d*-level spreading into a band of finite width W_d; B_d is the energy of the *d*-band bottom; and $n_d(E)$ is the density of electron states in the *d*-band.

Thus, to calculate the cohesive energy of transition metals and their alloys, it is necessary to know the density of electronic states $n_d(E)$ in the *d*-band. In the general case, the function $n_d(E)$ has a complicated form (there are minima

Donbass State Mechanical Engineering Academy, Kramatorsk. Translated from Poroshkovaya Metallurgiya, Vol. 47, No. 1–2 (459), pp. 37–54, 2008. Original article submitted December 3, 2007.

 1068-1302/08/0102-0026

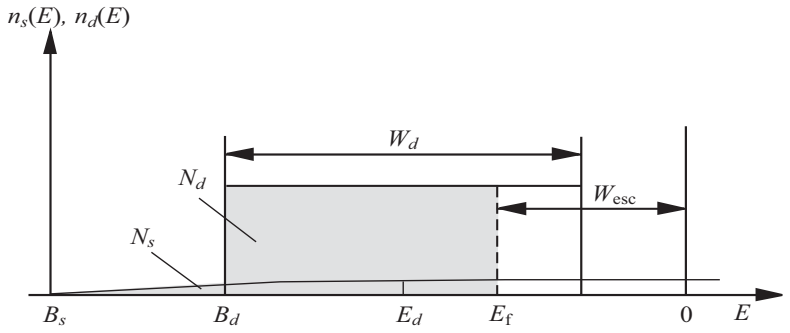

Fig. 1. Density of electron states of transition metals according to the Friedel model [7]

TABLE 1. Parameters of Band and Atomic Structure of Transition Metals [6]

Me	W_{esc}, eV	W_d, eV	E_d, eV	N_d	N_s	r_0, Å	R_d, Å
Sc	3.15	5.13	7.05	2.54	0.46	1.81	1.24
Ti	3.95	6.08	7.76	3.42	0.58	1.61	1.08
V	4.12	6.77	8.13	4.31	0.69	1.49	0.98
Cr	4.58	6.56	8.01	5.24	0.76	1.42	0.90
Mn	3.83	5.60	7.91	6.18	0.82	1.43	0.86
Fe	4.31	4.86	7.64	7.16	0.84	1.41	0.80
Co	4.41	4.35	7.36	8.16	0.84	1.39	0.76
Ni	4.50	3.78	6.91	9.19	0.81	1.38	0.71
Cu	4.40	2.80	5.90	10.0	1.00	1.41	0.67
Zn	4.24	–	–	–	2	1.52	–
Y	3.30	6.59	6.75	2.61	0.39	1.99	1.58
Zr	3.90	8.37	7.17	3.53	0.47	1.77	1.41
Nb	3.99	9.72	7.29	4.43	0.57	1.62	1.28
Mo	4.30	9.98	7.12	5.33	0.67	1.55	1.20
Tc	4.60	9.42	6.67	6.28	0.72	1.50	1.11
Ru	4.60	8.44	6.02	7.27	0.73	1.48	1.05
Rh	4.75	6.89	5.08	8.34	0.66	1.49	0.99
Pd	4.80	5.40	4.52	9.41	0.59	1.52	0.94
Ag	4.39	3.63	2.49	10.0	1.00	1.59	0.89
Cd	4.10	–	–	–	2	1.71	–
La	3.30	6.78	4.69	2.50	0.50	2.07	1.59
Hf	3.53	9.56	9.12	3.33	0.67	1.75	1.44
Ta	4.12	11.12	9.50	4.18	0.82	1.62	1.34
W	4.54	11.44	9.45	5.04	0.96	1.56	1.27
Re	5.00	11.02	8.99	5.96	1.04	1.52	1.20
Os	4.70	10.31	8.38	6.91	1.09	1.49	1.13
Ir	4.70	8.71	7.35	7.98	1.02	1.50	1.08
Pt	5.32	7.00	6.51	9.06	0.94	1.53	1.04
Au	4.30	5.28	5.18	10	1	1.59	1.01
Hg	4.52	–	–	–	2	1.78	–

and maxima), which primarily depends on the *d*-metal structure [6]. The complicated form of this function in the *d*-band can be modeled by constant density of states. Such a model was proposed by Friedel [7] where the density of states consists of (i) the density of *d*-type states located near the *d*-level energy E_d and being constant in a band of width W_d

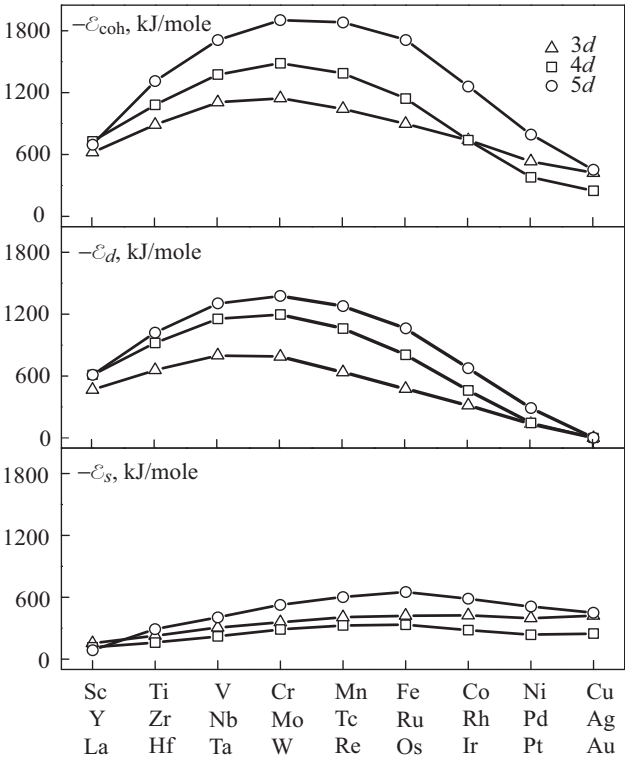

Fig. 2. Cohesive energy of transition metals and its *s*- and *d*-band components

corresponding to ten *d*-electrons per atom (Fig. 1) and (ii) the density of *s*-type states $n_s(E)$. The conduction-electron contribution to the cohesive energy can be calculated as follows [6]:

$$\boldsymbol{E}_s = \int_0^{E_f} E n_s(E) dE \,, \tag{2}$$

where $\boldsymbol{E}_s$ is the *s*-electron contribution to the cohesive energy, and $n_s(E)$ is the density of electron states in the conduction band, which can be found using the free-electron approximation [6]:

$$n_s(E) = \frac{2}{3\pi}\left(\frac{2m_e r_0^2}{\hbar^2\left(1+\dfrac{5r_d^3}{\pi r_0^3}\right)}\right)^{1.5} \sqrt{E} = R\sqrt{E} \,, \tag{3}$$

where r_0 is the atomic radius; r_d is the *d*-state radius; m_e is the electron mass; $\hbar$ is the Plank constant; and R is a parameter characterizing the density of states in the conduction band.

All the parameters needed to calculate the density of electronic states in the Friedel model (atomic radius r_0, *d*-state radius r_d, *d*-band width W_d, the number of *s*- and *d*-electrons N_s and N_d (Table 1)) are taken from [6], where these parameters were calculated and tabulated for all elements of the Periodic table using a single approach. This is why these parameters stand out among those obtained by fitting random experimental data and allow us to understand the basic laws governing the change of the electronic structure during transition from one metal to another.

Using the adopted form of the density of electronic states, we have calculated the cohesive energy of *d*-band, $\boldsymbol{E}_d$, and *s*-band, $\boldsymbol{E}_s$, and the total cohesive energy of transition metals, $\boldsymbol{E}_{\text{coh}}$. The calculated results are presented in Fig. 2 and Table 2 whence it follows that the cohesive energy $\boldsymbol{E}_{\text{coh}}$ of transition metals exhibits extreme behavior and has a

minimum, while the cohesive force peaks for chrome, molybdenum, and tungsten. The minima of the cohesive energy of these metals are associated with the maximum negative contribution of $\boldsymbol{E}_d$ for each of them in the corresponding transition row. According to Eq. (1), such values of $\boldsymbol{E}_d$ are due to the fact that the *d*-bands of chrome, molybdenum, and tungsten are almost half-complete. Figure 2 suggests that the term $\boldsymbol{E}_d$ has a considerable contribution to the total cohesive energy $\boldsymbol{E}_{\text{coh}}$ for the majority of transition metals. In each of the transitive rows, $\boldsymbol{E}_d$ decreases for metals of the eighth group and reaches zero for noble metals.

The contribution of *s*-electrons, $\boldsymbol{E}_s$, to the total cohesive energy $\boldsymbol{E}_{\text{coh}}$ is considerable and, for noble metals, is a unique source of cohesive force (Table 2). Figure 2 indicates that $\boldsymbol{E}_s$ varies nonmonotonically within the transition rows. It is minimum in absolute magnitude for the metals at the beginning of the transition row and increases to the end of the row, peaking for cobalt, ruthenium, and osmium. These values are due to the competition of two parameters determining the cohesive energy of the conduction band: the number of *s*-electrons N_s filling it and the parameter r_0 related to its depth B_s.

Cohesive energy and bond strength in crystals play a paramount role for the melting process in which the cohesive forces holding atoms in a crystal lattice must be overcome [8]. It is important that the role of the cohesive energy is most significant at high temperatures close to the melting points because the effect of defects in the crystal lattice on crystal strength considerably weakens under such conditions. That the melting process and the cohesive force are related is evidenced by a clear correlation between the melting point of transition metals T_{melt} [9] and the calculated values of cohesive energy (Fig. 3a). An important characteristic of the strength of interatomic bonds is the sublimation heat ΔH_{subl}, which is equal to the energy needed to transform one mole of solid substance into vapor consisting of neutral

TABLE 2. Cohesive Energy of Transition Metals and Its *s*- and *d*-Band Components

Me	$\boldsymbol{E}_s$, kJ/mole	$\boldsymbol{E}_d$, kJ/mole	$\boldsymbol{E}_{\text{coh}}$, kJ/mole
Sc	–154	–468	–622
Ti	–228	–659	–887
V	–306	–800	–1106
Cr	–359	–788	–1147
Mn	–406	–637	–1043
Fe	–422	–476	–898
Co	–424	–315	–739
Ni	–398	–136	–534
Cu	–422	0	–422
Y	–117	–612	–729
Zr	–161	–921	–1082
Nb	–222	–1156	–1378
Mo	–289	–1197	–1486
Tc	–328	–1060	–1388
Ru	–335	–807	–1142
Rh	–282	–460	–742
Pd	–235	–144	–379
Ag	–249	0	–249
La	–87	–613	–700
Hf	–291	–1023	–1314
Ta	–407	–1303	–1710
W	–527	–1378	–1905
Re	–604	–1278	–1882
Os	–652	–1061	–1713
Ir	–587	–676	–1263
Pt	–508	–287	–795
Au	–452	0	–452

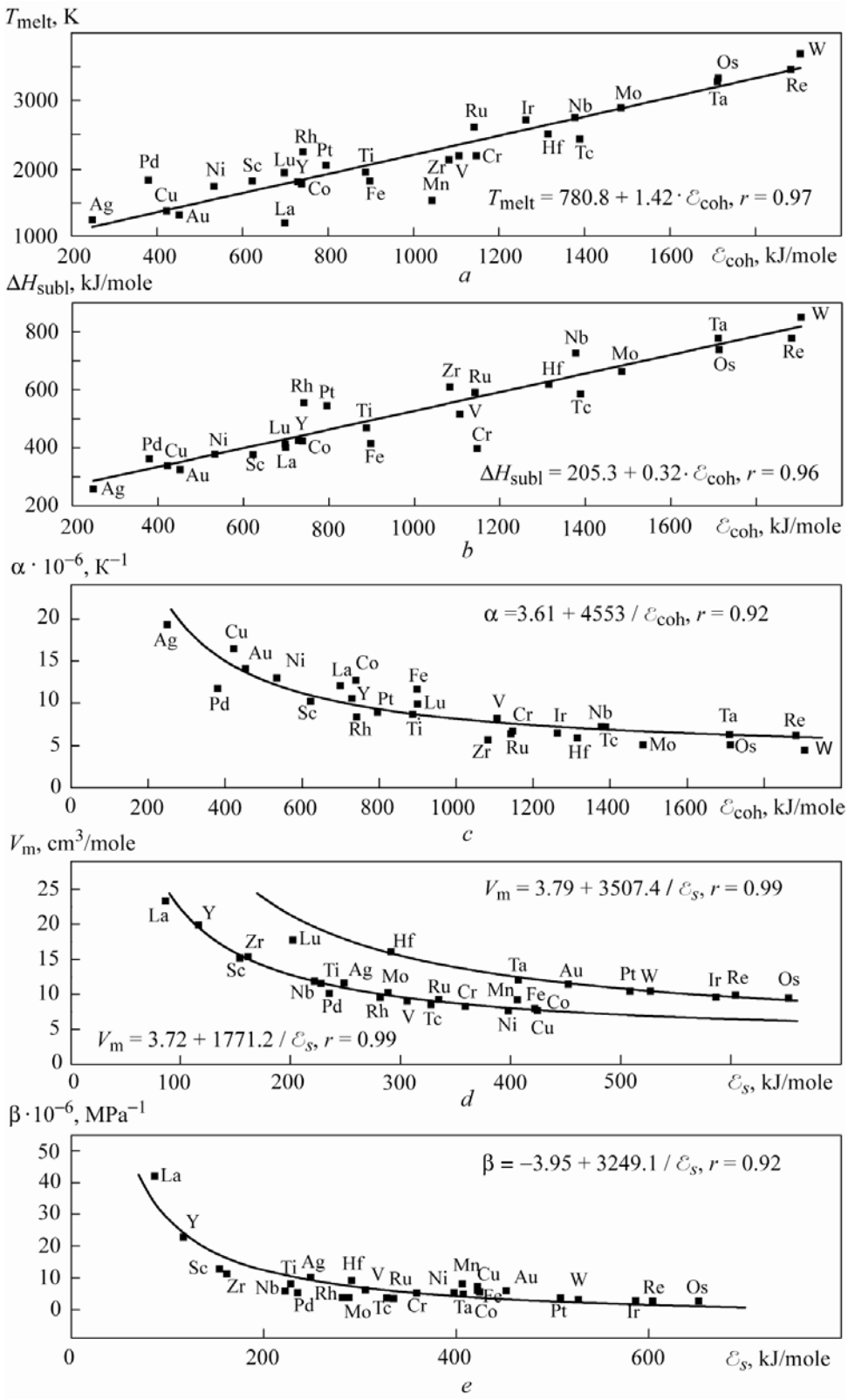

Fig. 3. Dependence of the properties of transition metals on the cohesive energy E_{coh} and the *s*-electron contribution E_s to it: *a*) T_{melt} on E_{coh}; *b*) ΔH_{subl} on E_{coh}; *c*) α on E_{coh}; *d*) V_m on E_s; *e*) β on E_s; the equations of fitting curves are given together with coefficients of correlation

atoms. Figure 3b shows the standard sublimation heats of transition metals [10] as functions of the cohesive energy. It should be noted that the strong correlation between these quantities allows us to consider the cohesive energy as a physical constant characterizing the strength of cohesive forces in metal.

Of the other characteristics dependent on the cohesive force and interatomic bond strength, we now consider the thermal expansion coefficient, which may be regarded as a measure of strength in the sense that the less this coefficient, the higher the resistance to the increase in the amplitude of thermal vibrations accompanying rise in temperature. In this case, the linear thermal expansion coefficient should be inversely proportional to the cohesive energy. Figure 3c shows how the linear thermal expansion coefficient α [11] depends on the cohesive energy. One might expect that the atomic mean-square displacements during thermal vibrations, as a characteristic of lattice strength, depend on the cohesive energy in a similar fashion.

One of the challenges attacked by solid-state physics is to establish the volume–energy relationship needed to calculate the equilibrium values of density, interatomic distances, and mole volumes. It should be noted that the roles of the *s*- and *d*-electrons are in direct opposition to each other. The band width W_d and, hence, the contribution of the *d*-electrons to the cohesive energy are strongly (as r^{-5}) dependent on the interatomic distance; therefore, the equilibrium volume appears much smaller than that obtained neglecting the effect the *d*-electrons [6]. Thus, transition metals are distinguished by strong compression of the *s*-states by the cohesive forces exerted by the *d*-electrons so that the *s*-electrons give one of the major contributions to the pressure, thus counterbalancing the attraction of the *d*-electrons [12]. Therefore, it is expedient to search for the relationship of the elastic constants and equilibrium mole volumes of transition metals with the contribution $\boldsymbol{E}_s$ of conduction electrons to the cohesive energy. Figure 3d shows the mole volume V_m of transition metals [11] as a function of $\boldsymbol{E}_s$. By the behavior of this dependence, there are two groups of transition metals. The mole volumes of the 3*d*- and 4*d*-transition metals can be related to $\boldsymbol{E}_s$ by the equation presented in Fig. 3d. Such values of $\boldsymbol{E}_s$ correspond to greater mole volumes of 5*d*-transition metals, which may be attributed to the fact that 4*f*-electron shells take part in the formation of atomic volumes in the metals of the fifth period. There is also stable correlation between the compressibility coefficient β [11] of transition metals and the *s*-electron contribution to the cohesive energy (Fig. 3e).

As for the properties of transition metals associated with the interatomic interaction in crystals, it should be pointed out that they are strongly correlated with the cohesive energy. After the above analysis, we can conclude that within a period the interatomic interaction, strength, and creep-resistance of *d*-metals increase in passing from the third to fifth group and then decrease in passing noble metals. This means that there is a certain pattern in how *d*-shells are filled as the atomic number increases, which results in extreme behavior of $\boldsymbol{E}_d$ within a period. In passing (within one group) from the third to the fifth period, the cohesive energy increases, which is consistent with the observed tendency to increase in their refractoriness and strength of interatomic bonds and may again be associated with the structure of the *d*-bands, namely, with their width.

It should be noted that $\boldsymbol{E}_d$ plays a decisive, but not unique (as pointed out in [2, 3]) role in the formation of the cohesive force. An analysis shows that each of the above quantities has stronger correlation with the cohesive energy $\boldsymbol{E}_\mathrm{coh}$ in comparison with $\boldsymbol{E}_d$. Hence, the effect of the *s*-electrons should be taken into account as a factor affecting the strength of transition metals. While the strength of interatomic bonds is determined by the joint contribution of the *s*- and *d*-electrons, the contribution of the *s*-electrons to the mole volume and compressibility is predominant.

COHESIVE ENERGY OF TRANSITION METALS ALLOY AND BEHAVIOR OF ALLOY FORMATION ENERGY

The contribution of electron transfer during alloying to the alloy formation energy can be calculated in the Hartree–Fock approximation as the difference between the cohesive energies of alloy A–B and its components A and B [2]:

$$\Delta H_1 = \boldsymbol{E}_\mathrm{coh}^\mathrm{all} - x_\mathrm{A}\boldsymbol{E}_\mathrm{coh}^\mathrm{A} - x_\mathrm{B}\boldsymbol{E}_\mathrm{coh}^\mathrm{B}, \quad (4)$$

where ΔH_1 is the contribution to the enthalpy of formation of the alloy A–B; x_i are the mole fractions of the alloy components; and $\boldsymbol{E}_\mathrm{coh}^\mathrm{all}$, $\boldsymbol{E}_\mathrm{coh}^\mathrm{A}$, $\boldsymbol{E}_\mathrm{coh}^\mathrm{B}$ are the cohesive energies of the alloy and its components.

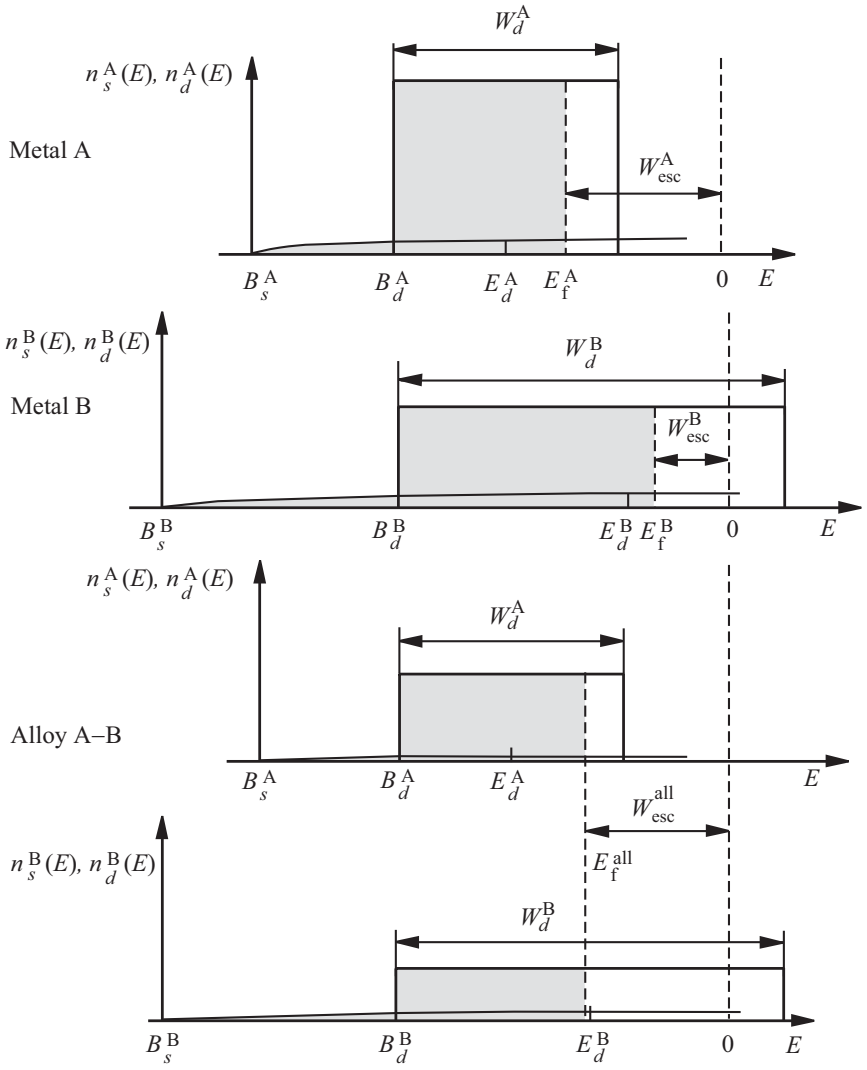

Fig. 4. Density of electron states of pure components and equiatomic alloy: the electron-band parameters of the components remain the same in the alloy

In [4, 5, 13, 14], the contribution $\boldsymbol{E}_d$ was considered unique in calculating the heat of formation of disordered alloys of transition metals. The participation of the *s*-electrons in the formation of cohesion was not disregarded. However, the contribution of the *s*-electrons to $\boldsymbol{E}_{\mathrm{coh}}$ calculated in the first part of the present paper indicate that both contributions $\boldsymbol{E}_d$ and $\boldsymbol{E}_s$ to the cohesive energies of the components and to the cohesive energy of the alloy should be accounted for in calculating the contribution ΔH_1 to the enthalpy of formation of the alloy, according to Eq. (4). In calculating the cohesive energy of the alloy, an important problem is to model the density of electronic states of the alloy. One of the goals set here is to calculate the density of electronic states of an alloy from the electron-band parameters of its components.

Let us examine an alloy band formation scenario in which the densities of electronic states due to the pure components are constant before and after alloy formation. This scenario is illustrated in Fig. 4. The form of density of electronic states of the alloy can be calculated from those of pure metals:

$$n_{\mathrm{all}}(E) = x_{\mathrm{A}} n_{\mathrm{A}}(E) + x_{\mathrm{B}} n_{\mathrm{B}}(E)\,. \tag{5}$$

In calculating the cohesive energies of metals and alloys, the values of the energy E should be reckoned from one level, say, electron energy in vacuum, which is convenient. Then the cohesive energy can be calculated from the following formulas.

For the pure component A —

$$\boldsymbol{E}_{\text{coh}}^{\text{A}} = \int_{E_d^{\text{A}} - \frac{W_d^{\text{A}}}{2} - E_{\text{f}}^{\text{A}} - W_{\text{esc}}^{\text{A}}}^{-W_{\text{esc}}^{\text{A}}} (E_d^{\text{A}} - E - E_{\text{f}}^{\text{A}} - W_{\text{esc}}^{\text{A}}) n_d^{\text{A}}(E) dE + \int_{B_s^{\text{A}}}^{-W_{\text{esc}}^{\text{A}}} R^{\text{A}} (E - E_{\text{f}}^{\text{A}} - W_{\text{esc}}^{\text{A}})^{1.5} dE , \tag{6}$$

where W_d^{A} is the width of the d-band of the metal A; E_d^{A} is the energy of the d-level of the metal A; E_{f}^{A} is the Fermi energy of the metal A reckoned from the conduction-band bottom; $W_{\text{esc}}^{\text{A}}$ is the electronic work function of the metal A; R^{A} is a parameter characterizing the density of electron states in the conduction band of the metal A; n_d^{A} is the density of electron states in the d-band of the transition metal A; and B_s^{A} is the energy of the conduction-band bottom of the metal A.

For the pure component B —

$$\boldsymbol{E}_{\text{coh}}^{\text{B}} = \int_{E_d^{\text{B}} - \frac{W_d^{\text{B}}}{2} - E_{\text{f}}^{\text{B}} - W_{\text{esc}}^{\text{B}}}^{-W_{\text{esc}}^{\text{B}}} (E_d^{\text{B}} - E - E_{\text{f}}^{\text{B}} - W_{\text{esc}}^{\text{B}}) n_d^{\text{B}}(E) dE + \int_{B_{\text{s}}^{\text{B}}}^{-W_{\text{esc}}^{\text{B}}} R^{\text{B}} (E - E_{\text{f}}^{\text{B}} - W_{\text{esc}}^{\text{B}})^{1.5} dE , \tag{7}$$

where W_d^{B} is the width of the d-band of the metal B; E_d^{B} is the energy of the d-level of the metal B; E_{f}^{B} is the Fermi energy of the metal A reckoned from the conduction-band bottom B_s^{B}; $W_{\text{esc}}^{\text{B}}$ is the electronic work function of the metal B; R^{B} is a parameter characterizing the density of electron states in the conduction band of the metal B; and n_d^{B} is the density of electron states in the d-band of the transition metal B.

For the component A in alloy —

$$\boldsymbol{E}_{\text{coh}}^{\text{A, all}} = \int_{E_d^{\text{A}} - \frac{W_{\text{d}}^{\text{A}}}{2} - E_{\text{f}}^{\text{all}} - W_{\text{esc}}^{\text{all}}}^{-W_{\text{coh}}^{\text{all}}} (E_d^{\text{A}} - E - E_{\text{f}}^{\text{all}} - W_{\text{esc}}^{\text{all}}) n_d^{\text{A}}(E) dE + \int_{B_{\text{s}}^{\text{A}}}^{-W_{\text{esc}}^{\text{all}}} R^{\text{A}} (E - E_{\text{f}}^{\text{all}} - W_{\text{esc}}^{\text{all}})^{1.5} dE , \tag{8}$$

where $W_{\text{esc}}^{\text{all}}$ is the electronic work function of the alloy A–B, and $E_{\text{f}}^{\text{all}}$ is the Fermi energy of the alloy A–B reckoned from the conduction-band bottom.

For the component B in alloy —

$$\boldsymbol{E}_{\text{coh}}^{\text{B, all}} = \int_{E_d^{\text{B}} - \frac{W_d^{\text{B}}}{2} - E_{\text{f}}^{\text{all}} - W_{\text{esc}}^{\text{all}}}^{-W_{\text{esc}}^{\text{all}}} (E_d^{\text{B}} - E - E_{\text{f}}^{\text{all}} - W_{\text{esc}}^{\text{all}}) n_d^{\text{B}}(E) dE + \int_{B_s^{\text{B}}}^{-W_{\text{esc}}^{\text{all}}} R^{\text{B}} (E - E_{\text{f}}^{\text{all}} - W_{\text{esc}}^{\text{all}})^{1.5} dE . \tag{9}$$

The Fermi energy of the alloy A–B $E_{\text{f}}^{\text{all}}$ can be calculated from the normalization condition for the functions $n_s(E)$ and $n_d(E)$:

$$x_{\text{A}}(N_s^{\text{A}} + N_d^{\text{A}}) + x_{\text{B}}(N_{\text{s}}^{\text{B}} + N_{\text{d}}^{\text{B}}) = \sum_{i=\text{A,B}} \left[\int_{B_s^i}^{E_{\text{f}}^{\text{all}}} n_s^i(E) dE + \int_{B_d^i}^{E_{\text{f}}^{\text{all}}} n_d^i(E) dE \right], \tag{10}$$

where N_s^{A}, N_d^{A}, N_s^{B}, and N_d^{B} are the number of s- and d-electrons in the pure components A and B, respectively.

Then resultant expression for the contribution ΔH_1 due to electron transfer during alloy formation becomes

$$\Delta H_1 = x_{\text{A}}(\boldsymbol{E}_{\text{coh}}^{\text{A, all}} - \boldsymbol{E}_{\text{coh}}^{\text{A}}) + x_{\text{B}}(\boldsymbol{E}_{\text{coh}}^{\text{B, all}} - \boldsymbol{E}_{\text{coh}}^{\text{B}}). \tag{11}$$

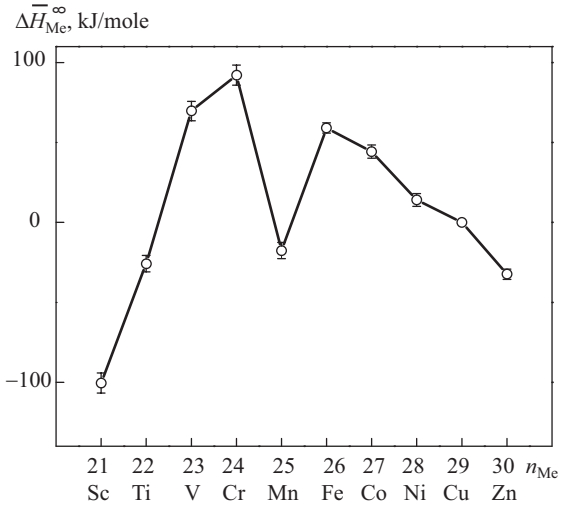

Fig. 5

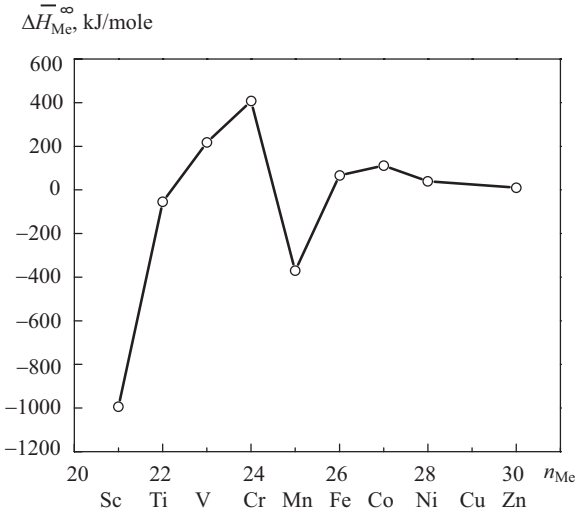

Fig. 6

Fig. 5. First mixing enthalpy of 3*d*-metals $\Delta\overline{H}^{\infty}_{Me}$ (kJ/mole) in liquid Cu–3*d*-metal alloys as a function of the atomic number of the 3*d*-metal

Fig. 6. First mixing enthalpy (kJ/mole) of 3*d*-metals and cuprum calculated by formula (5)

The other contribution to the enthalpy of alloy formation is due to the difference between the *d*-band widths of the pure metals [2]:

$$\Delta H_2 = x_A x_B (W_d^B - W_d^A)\left(\frac{E_{coh}^B}{W_d^B} - \frac{E_{coh}^A}{W_d^A}\right). \quad (12)$$

This contribution is always positive, and its concentration dependence is symmetric about the equiatomic composition. When the widths of the *d*-bands of the component metals are equal, this contribution tends to zero.

The contributions ΔH_1 and ΔH_2 can be used to calculate the mixing enthalpy of the components:

$$\Delta H = \Delta H_1 + \Delta H_2.$$

Whether the above considerations are correct can be checked in calculating the state variables of the formation of disordered alloys of transition metals, such as mixing enthalpies of liquid alloys. The modern literature provides detailed experimental data on ΔH of liquid Cu–3*d*-metal alloys. The thermodynamic properties of liquid binary alloys of copper and 3*d*-metals depend in a complicated manner on the position of the components in the Periodic Table [15]. Figure 5 shows the first mixing enthalpies of 3d-metals and copper. The negative deviations from ideality in Cu–Sc and Cu–Ti melts, which are indicative of preferential interaction of unlike atoms, are succeeded by positive deviations from ideality in the Cu–V and Cu–Cr systems, which are indicative of the intensive interaction of like atoms. In Cu–Mn melts, the interparticle interaction of unlike atoms is more intensive, which results in sign-variable concentration dependence of excess thermodynamic functions of mixing. In going to Cu–Fe melts, the interaction of like atoms intensifies, resulting in positive deviations of the thermodynamic properties from ideality. In Cu–Fe → Cu–Co → Cu–Ni, the interaction of like atoms in melt is weaker, since the positive deviations of the thermodynamic functions of mixing from ideality decrease and then become negative for the Cu–Zn system.

An analysis shows that it is possible to qualitatively interpret the above behavior of the mixing enthalpy of Cu–3*d*-metal melts. Figure 6 demonstrates the first mixing enthalpy of 3*d*-metals and copper. Comparing these calculated data with the experimental values in Fig. 5, we can conclude that the above procedure makes it possible to interpret qualitatively the exothermic mixing enthalpies of copper with scandium and titanium as well as the positive mixing enthalpies of vanadium and chrome, the exothermicity of the first mixing enthalpy of manganese, and the decrease in the first mixing enthalpies for elements of the row from iron to zinc.

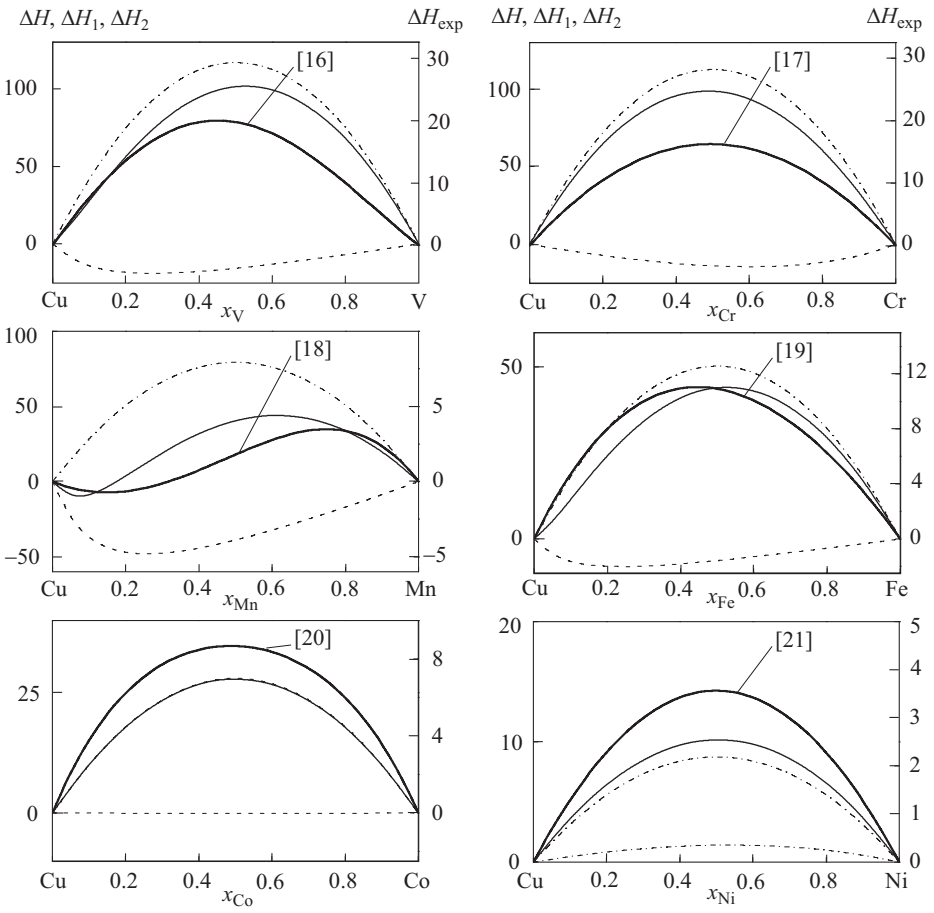

Fig. 7. Theoretical concentration dependence of the mixing enthalpies (kJ/mole) of binary alloys of cuprum with vanadium, chromium, manganese, iron, cobalt, and nickel: solid line denotes ΔH, dashed line denotes ΔH_1, dash-and-dot line denotes ΔH_2, solid heavy line denotes ΔH_{exp} according to the reference

Table 3 summarizes the calculated contributions $\Delta\overline{H}_1^{\infty}$ and $\Delta\overline{H}_2^{\infty}$ as well as the calculated first mixing enthalpies of the components, $\Delta\overline{H}_{Me}^{\infty}$. That the calculated first mixing enthalpy in some cases differs by several times in absolute magnitude from the experimental values should not be seen as a bad result. First, the calculations have been conducted ab initio, and none of the contributions was somehow normalized or adjusted. Second, the calculated mixing

TABLE 3. First Mixing Enthalpy of *d*-Metals and Cuprum and Its Contributions Calculated by Formula (5)

Me	$\Delta\overline{H}_1^{\infty}$, kJ/mole	$\Delta\overline{H}_2^{\infty}$, kJ/mole	$\Delta\overline{H}_{Me}^{\infty}$, kJ/mole
Sc	–1205	211	–994
Ti	–407	352	–55
V	–247	464	217
Cr	–40	447	407
Mn	–685	315	–370
Fe	–132	200	68
Co	0	111	111
Ni	5	35	40
Zn	11	0	11

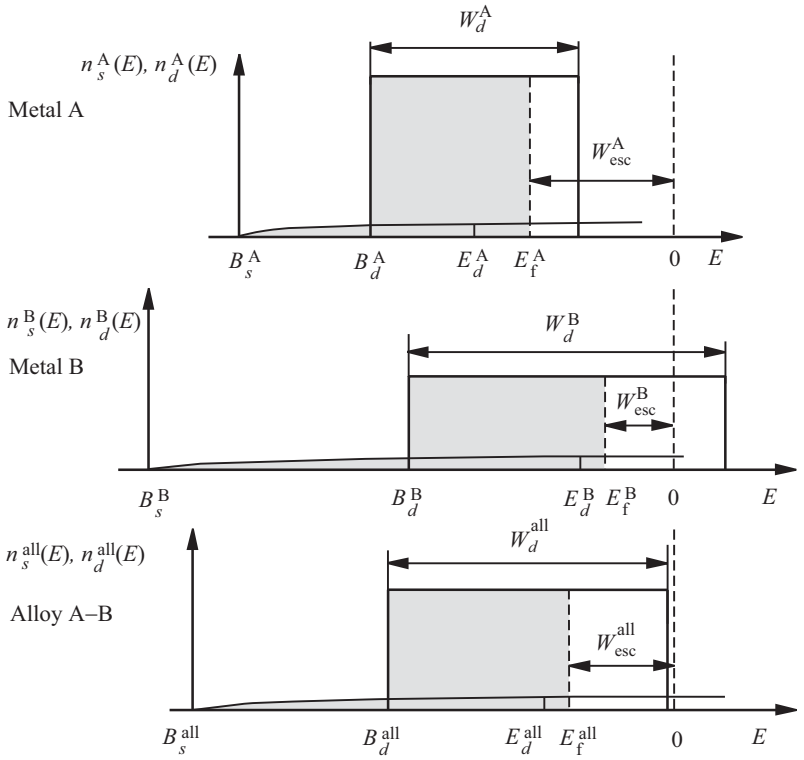

Fig. 8. Density of electron states of pure components and alloy with equiatomic composition: the electron-band parameters of the alloy differ from those of its components

enthalpies have been found as the difference between large numbers, which always has an adverse effect in calculations. Third, the calculations allow us to reproduce not only the variation of the properties of a number of systems as a whole, but also correctly reproduce the concentration dependence of the mixing enthalpy for Cu–V, Cu–Cr, Cu–Mn, Cu–Fe, Cu–Co, and Cu–Ni alloys (Fig. 7). As follows from the figure, the positive mixing enthalpy in the Cu–V and Cu–Cr systems is due primarily to the large positive contribution ΔH_2 associated with the considerable difference of W_d of the components. In contrast, the contribution ΔH_1 appears small because the transition of electrons from the energy levels of vanadium or chrome to those of copper leads to decrease in N_d at the levels of vanadium and chrome in the alloy and, hence, to decrease in the terms $\boldsymbol{E}_{\mathrm{coh}}^{\mathrm{V,all}}$ and $\boldsymbol{E}_{\mathrm{coh}}^{\mathrm{Cr,all}}$. The sign-variable mixing enthalpy of the Cu–Mn system can be attributed to the competition of ΔH_1 and ΔH_2 different in sign, but comparable in absolute magnitude. In the Cu–Fe, Cu–Co, and Cu–Ni systems, positive mixing enthalpies are associated with the contribution ΔH_2, while the contribution ΔH_1 decreases in absolute magnitude.

The above approach failed to reproduce the concentration dependence of the mixing enthalpy for the Cu–Sc and Cu–Ti systems. For the Cu–Sc system, formula (5) yields negative mixing enthalpy over the entire range of structures, but the minimum shifts toward copper-rich alloys. For the Cu–Ti system, the mixing enthalpy appears positive for titanium-rich alloys. An analysis of Table 1 reveals a considerable difference of the electronic work functions and the widths of the *d*-bands of the components of the Cu–Sc and Cu–Ti systems. With such a combination of the electron-band parameters of the components, formula (5) used to calculate the density of electronic states of alloys may not account for features of interaction in the system. In this connection, we analyzed another scenario in which the electron-band parameters of the alloy differ from those of the pure component metals.

One of the possibilities is to find the electron-band parameters of an alloy from those of the pure metals by using an additive model (Fig. 8) in which the density of electron states in an alloy is calculated as

$$n^{\mathrm{all}}(E) = n_s^{\mathrm{all}}(E) + n_d^{\mathrm{all}}(E), \tag{13}$$

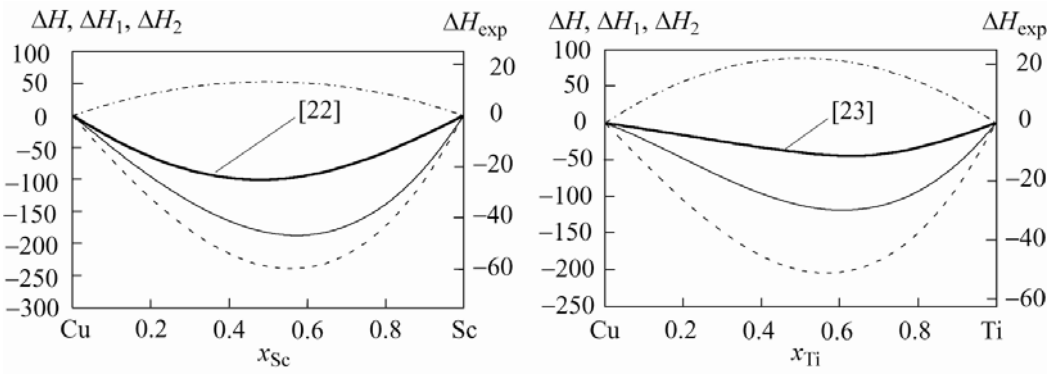

Fig. 9. Theoretical concentration dependence of the mixing enthalpies (kJ/mole) of binary alloys of cuprum with scandium and titanium: solid line denotes ΔH, dashed line denotes ΔH_1, dash-and-dot line denotes ΔH_2, solid heavy line — ΔH_{exp} according to the reference

where

$$n_s^{\text{all}}(E) = (x_{\text{A}} \cdot R^{\text{A}} + x_{\text{B}} \cdot R^{\text{B}})\sqrt{E} \tag{14}$$

is the density of states of conduction electrons in the alloy; R^{A} and R^{B} are parameters defining the form of the density functions for electron states in the conduction bands of the alloy components;

$$n_d^{\text{all}}(E) = 10/\left[x_{\text{A}} W_d^{\text{A}} + x_{\text{B}} W_d^{\text{B}}\right] \tag{15}$$

is the density of states in the *d*-band of the alloy. The energy of the atomic *d*-level of the alloy is defined by

$$E_d^{\text{all}} = x_{\text{A}} E_d^{\text{A}} + x_{\text{B}} E_d^{\text{B}}. \tag{16}$$

The Fermi energy can be calculated from the normalization condition

$$x_{\text{A}}(N_s^{\text{A}} + N_d^{\text{A}}) + x_{\text{B}}(N_s^{\text{B}} + N_d^{\text{B}}) = \int_{B_s^{\text{all}}}^{E_{\text{f}}^{\text{all}}} n_{\text{s}}^{\text{all}}(E)dE + \int_{B_d^{\text{all}}}^{E_{\text{f}}^{\text{all}}} n_d^{\text{all}}(E)dE. \tag{17}$$

The energy of the conduction-band bottom of the alloy can also be calculated by the additive model:

$$B_{\text{s}}^{\text{all}} = x_{\text{A}} B_{\text{s}}^{\text{A}} + x_{\text{B}} B_{\text{s}}^{\text{B}}. \tag{18}$$

In this case, the cohesive energy of the alloy can be calculated as

$$E_{\text{coh}}^{\text{all}} = \int_{E_d^{\text{all}} - \frac{W_d^{\text{all}}}{2} - E_{\text{f}}^{\text{all}} - W_{\text{esc}}^{\text{all}}}^{-W_{\text{esc}}^{\text{all}}} (E_d^{\text{all}} - E - E_{\text{f}}^{\text{all}} - W_{\text{esc}}^{\text{all}}) n_d^{\text{all}}(E)dE + \int_{B_s^{\text{all}}}^{-W_{\text{esc}}^{\text{all}}} R^{\text{all}}(E - E_{\text{f}}^{\text{all}} - W_{\text{esc}}^{\text{all}})^{1.5} dE. \tag{19}$$

The contributions ΔH_1 and ΔH_2 to the mixing enthalpy of the alloy have been calculated using formulas (4) and (12), respectively. The use of the second scenario to calculate the first mixing enthalpies of 3*d*-metals with copper shows that this model gives a worse fit to the experimental behavior values for a number of systems. At the same time, the first mixing enthalpy (–500 kJ/mole) of scandium appears closer to the experimental value. Moreover, such an analysis makes it possible to correctly interpret the concentration dependence of integral mixing enthalpy for the Cu–Sc and Cu–Ti systems (Fig. 9). The calculated minimum of ΔH shifts toward titanium-rich alloys for the Cu–Ti system and toward the equiatomic composition for the Cu–Sc system. According to the calculations, the exothermic mixing enthalpies in these systems are primarily determined by the contribution ΔH_1 associated with the transition of electrons from the energy levels of scandium and titanium to those of copper during alloy formation.

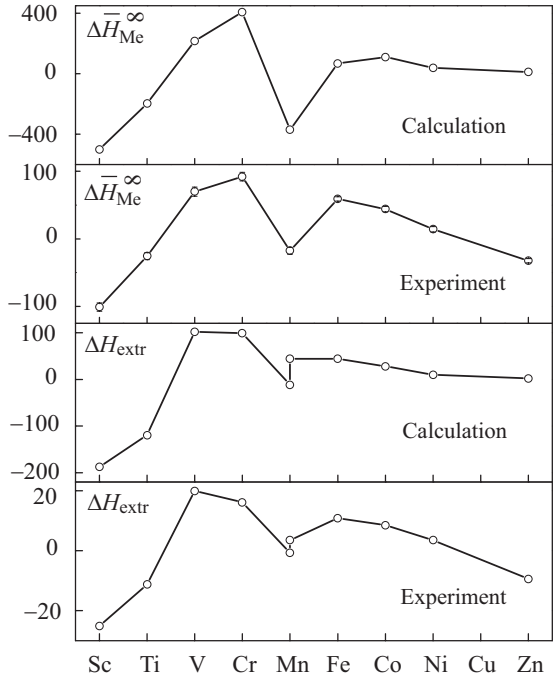

Fig. 10. Theoretical and experimental [15] values of the first mixing enthalpy (kJ/mole) and integral mixing enthalpy (kJ/mole) of 3*d*-metals with cuprum

An analysis of the calculated results for Cu–3*d*-metal systems reveals that for alloys whose components have similar electron-band parameters, the model in Fig. 4 is preferable to assess the mixing enthalpies, while expression (11) is preferable to calculate the contribution ΔH_1. If an alloy has components with considerably different electron-band parameters, it is expedient to use the model in Fig. 8.

The calculated values of the first mixing enthalpies of the components and the extreme values of the integral mixing enthalpy obtained as described above are compared with experimental data in Fig. 10. It is easy to notice that by introducing a normalization constant of about 4, we can achieve not only qualitative, but also quantitative agreement between the experimental and calculated values. The agreement between the calculated and experimental dependences indicates that the two contributions ΔH_1 and ΔH_2 taken into account here are indeed decisive, and the models proposed can be used to interpret the interaction of the components in other systems or rows of systems based on transition metals. Further efforts to improve the above method of calculating the energy contributions to the enthalpies of formation of disordered alloys for the purpose of achieving not only qualitative, but also quantitative agreement between the calculated and experimental values will go into the refinement of the electron-band parameters of alloys and their components, the use of more complicated forms of the density of electronic states in the *d*-band, the incorporation of some other energy contributions, say, the contribution due to the electron–phonon interaction, etc.

CONCLUSIONS

We used tight-binding and Friedel's model for the density of electronic states to calculate the cohesive energy of transition metals and its *s*- and *d*-electron contributions. It has been shown that the strength of interatomic bonds, mole volume, and compressibility of transition metals correlate with the cohesive energy and its contributions. The important role of conduction electrons in the formation of cohesive force of transition metals has been shown.

The major contributions to the formation energy of disordered alloys of copper with transition metals have been calculated. It has been shown that the mixing enthalpy of alloys can be represented as the sum of a negative contribution due to electron transitions during alloy formation and positive contribution due to the difference between the widths of the *d*-bands of the pure components.

The calculated results are in qualitative agreement with the experimental data on the behavior of thermodynamic properties in the Cu–3*d*-metal systems considered and on the experimental concentration dependence of the thermodynamic properties.

REFERENCES

1. G. V. Samsonov, I. F. Prydko, and L. F. Pryadko, *Electron Localization in Solids* [in Russian], Nauka, Moscow (1976), p. 339.
2. M. Cyrot M and F. Cyrot-Lackmann, "Energy of formation of binary transitional alloys," *J. Phys. F: Metal Phys.*, **6**, No. 12, 2257–2265 (1976).
3. D. G. Pettifor, "Theory of energy bands and related properties of 4*d* transition metals. III. S and d-contributions to the equation of state," *J. Phys.*, **F8**, No. 2, 219–230 (1978).
4. A. Pasturel, C. Colinet, and P. Hicter, "Heats of formation in transition intermetallic alloys," *Acta Metall.*, **32**, No. 7, 1061–1067 (1984).
5. D. G. Pettifor, "On the tight binding theory of the heats of formation," *Sol. State Com.*, **28**, 621–623 (1978).
6. W. A. Harrison, *Electronic Structure and the Properties of Solids*, Freeman, New York, (1980).
7. J. Friedel, *The Physics of Metals*, Cambridge University Press, New York (1969), p. 512.
8. Ya. P. Frenkel', *An Introduction to the Theory of Metals* [in Russian], Metallurgizdat, Moscow (1972), p. 424.
9. A. T. Dinsdale, "SGTE data for pure elements," *CALPHAD*, **15**, No. 4, 317–425 (1991).
10. J. A. Dean (ed.), *Lange's Handbook of Chemistry*, McGraw-Hill, New York (1999), p. 1291.
11. E. M. Sokolovskaya and L. S. Guzei, *Metal Chemistry* [in Russian], Izd. Mosk. Univ., Moscow (1986), p. 264.
12. D. G. Pettifor, "*S*- and *d*-contributions to the transition metal equation of state," in: *Proc. Int. Conf. Transit. Metals* (Toronto, 1977), Bristol–London (1978), pp. 6–13.
13. D. G. Pettifor, "Theory of the heats of formation of transition-metal alloys," *Phys. Rev. Lett.*, **42**, No. 13, 846–849 (1979).
14. A. Pasturel, P. Hicter, and F. Cyrot-Lackmann, "Heats of formation of binary transition metal alloys," *Sol. State Comm.*, **48**, No. 6, 561–562 (1983).
15. M. A. Turchanin, "Enthalpy of formation of liquid alloys of cuprum and 3*d*-transition metals," *Metally*, No. 4, 22–28 (1998).
16. M. A. Turchanin, "Phase equilibria and thermodynamics of binary copper systems with 3*d*-metals. II. The copper–vanadium system," *Powder Metall. Met. Ceram.*, **45**, No. 5-6, 272–278 (2006).
17. M. A. Turchanin, "Phase equilibria and thermodynamics of binary copper systems with 3d-metals. III. Copper–chromium system," *Powder Metall. Met. Ceram.*, **45**, No. 9–10, 457–467 (2006).
18. M. A. Turchanin, P. G. Agraval, and A. R. Abdulov, "Phase equilibria and thermodynamics of binary copper systems with 3*d*-metals. IV. Copper–manganese system," *Powder Metall. Met. Ceram.*, **45**, No. 11–12, 569–581 (2006).
19. M. A. Turchanin, "Thermodynamics of liquid alloys, and stable and metastable phase equilibria in the copper–iron system," *Powder Metall. Met. Ceram.*, **40**, No. 7–8, 337–353 (2001).
20. M. A. Turchanin and P. G. Agraval, "Phase equilibria and thermodynamics of binary copper systems with 3*d*-metals. V. Copper–cobalt system," *Powder Metall. Met. Ceram.*, **46**, No. 1–2, 77–89 (2007).
21. M. A. Turchanin, P. G. Agraval, and A. R. Abdulov, "Phase equilibria and thermodynamics of binary copper systems with 3*d*-metals. VI. Copper–nickel system," *Powder Metall. Met. Ceram.*, **46**, No. 9–10, 467–477 (2007).
22. M. A. Turchanin, "Phase equilibria and thermodynamics of binary copper systems with 3*d*-metals. I. The copper–scandium system," *Powder Metall. Met. Ceram.*, **45**, No. 3–4, 143–152 (2006).
23. M. A. Turchanin, P. G. Agraval, A. N. Fesenko, and A. R. Abdulov, "Thermodynamics of liquid alloys and metastable phase transformations in the copper–titanium system," *Powder Metall. Met. Ceram.*, **44**, No. 5–6, 259–270 (2005).